CFD Modeling of Air Pollution Dispersion in Complex Urban Area

Mohamed S. Idrissi, Fatma A. Lakhal, Nabil Ben Salah and Mouldi Chrigui

Abstract With the ultimate goal of prediction species dispersion and pollution transport using computational fluid dynamics (CFD), this paper evaluates the performance of two different modeling approaches Reynolds-averaged Navier–Stokes (RANS) standard k-e, and Large Eddy Simulation (LES) applied to pollutant dispersion in an actual urban environment downtown Hannover. The modeling is based on the hypothesis neutral atmospheric conditions. LES is chosen to capture the effects of velocity randomness of the pollutants convection and diffusion. Computer-aided design, CAD, of Hannover city demonstrating different topologies and boundaries conditions, are cleaned, then in fine grids meshed. Pollutants are introduced into the computational domain through the chimney and/or pipe leakages. Weather conditions are accounted for using logarithmic velocity profiles at inlets. Simulations are conducted on 80 cores cluster for several days. CH_4 distributions as well as streamlines and velocity profiles conducted on reasonable results. The major interest of presenting work is that it involved a large group of real buildings with a high level of details that can represent the real case of the problem.

M. S. Idrissi (✉) · F. A. Lakhal · M. Chrigui
Research Unit "Materials, Energy and Renewable Energies", Gafsa Faculty of Science,
University Campus Sidi Ahmed Zarroug Gafsa, 2112 Gafsa, Tunisia
e-mail: idrissimedsalah@gmail.com

M. Chrigui
e-mail: mouldi.cherigui@gmx.de

M. S. Idrissi · F. A. Lakhal · M. Chrigui
Research Unit "Mechanical Modeling Materials, Energy", National school
of engineer of Gabes, 6029 Zrig Gabes, Tunisia

N. B. Salah · M. Chrigui
CADFEM AN, Sousse Techn022e, Sousse, Tunisia

M. Chrigui
Department of Mechanical Engineering, Institute for Energy and Power Plant Technology,
Technische Universität Darmstadt, Petersenstr.30, 64287 Darmstadt, Germany

Nomenclature

Acronym

CFD   Computational Fluid Dynamics
DNS   Direct Numerical Simulation
LES   Large Eddy Simulation
RANS   Reynolds-Averaged Navier–Stokes
SST   Shear Stress Transport
URANS   Unsteady Reynolds-Averaged Navier–Stokes

Greek symbols

μ Dynamic viscosity Ns m^{-2}
v Kinematic viscosity m^2 s^{-1}
ω Specific turbulence dissipation s^{-1}
R   Rate
τ_{ij} Unresolved stress tensor kg m^{-1} s^{-2}
ε Turbulence dissipation m^2 s^{-3}

Mathematical symbols

∇ Nabla operator

Roman symbols

$\bar{u}$ Filtered velocity m s^{-1}
f   Body forces per unit volume N m^{-3}
u   Fluid flow velocity m s^{-1}
ρ Density kg m^{-3}
e   Total specific internal energy m^2 s^{-2}
k   Turbulence kinetic energy m^2 s^{-2}
p   Pressure N m^{-2}
q   Energy source term m^2 s^{-2}
t   Time s
U   Mean velocity m s^{-1}
$u^{'}$ Fluctuating part of velocity m s^{-1}
x   Position vector m

1   Introduction

Air quality has a great importance in urban complexes because of the several effects on human safety and environment. The growth of urbanization puts a pressure on urban stocks, appear in augmented use of a vehicle and a denser urban fabric.

Climate, city and the nontrivial combine of pollutant sources cause high pedestrian level concentrations. Thus, it is indispensable that novel simulation tools are advanced and current methods are upgraded to aid controllers and urban designers to reduce air pollution problems in cities, and to permit emergency establishments to plan evacuation strategies ensuing accidents, deliberate release of the dangerous airborne substance or natural catastrophes, (Salim et al. 2011).

Nowadays computational fluid dynamics (CFD) is quickly imposing itself also in the air pollution dispersion in an urban area, (DeCroix and Brown 2002). Contrary to most currently usual air quality models, CFD simulations can estimate rigorously topographical details such as terrain variations and building structures in urban areas along with local aerodynamics and turbulence, (Tang et al. 2005). CFD is a numerical resolution of the fundamental physics equations and contains the effects of detailed three-dimensional geometry and local environmental conditions. Therefore, it is able to provide more precise solutions than statutory existing models of air quality (Huber et al. 2004), because Many works can be found in the literature reporting on the use of (CFD) techniques to model flow and pollutant dispersion around isolated buildings or groups of buildings (Blocken et al. 2012; Breuer et al. 2003; Chan et al. 2002; Tominaga and Stathopoulos 2010; Kikumoto and Ooka 2012). However, gas dispersion in complexes urban areas is still limited to isolated cases and to a limited number of sources.

In this work, the focus is put on the investigation of pollutants transport and dispersion which exhibit complex geometries and diverse boundary conditions. Diverse scenarios of pollutants injection into the computational domain are studied. In the following, an introduction of the work including used physics and choosed geometries is presented, then details about generated grid and applied boundary conditions are explained. In the third part, discussion and presentation of obtained results is given. At the end of the report, a conclusion is included.

2 Modeling

2.1 *Governing Equations*

Known as Navier–Stokes equations, the fundamental governing equations of fluid flow are the base of the CFD. They are partial differential equations expressing three basic physical rules: the conservation of mass (1) the Newton's Law of Motion (2) and the conservation of energy (3), Wendt et al. (1996).

$$\frac{\partial p}{\partial t} + \nabla \cdot \rho u = 0 \tag{1}$$

$$\frac{\partial pu}{\partial t} + \nabla \cdot (\rho uu) = -\nabla p + \nabla(\mu \nabla u) + f \tag{2}$$

$$\frac{\partial pe}{\partial t} + \nabla \cdot (\rho u e) = -\nabla pu + \nabla \cdot (\mu u \nabla) - \nabla q \tag{3}$$

The direct numerical simulation (DNS) is a numerical integration of the Navier–Stokes equations that directly solves the flow without any modeling, and captures all the spatial and temporal scales of the flow. Its power is to produce exact, analytic resolutions unaffected by estimates, at the whole computational domain and all times of the simulated period necessitates a high-resolution grid and costs enormous calculating resources and time, avoiding DNS from being applied in complex urban environment problems and in wind engineering, Rudman and Blackburn (2006). When the time-dependent equations are solved on a very coarse grid that does not capture the small scales of the flow. This approach is called large eddy simulation (LES) (4), (Moin and Mahesh 1998).

$$\frac{\partial \overline{u_i}}{\partial t} + \frac{\partial}{\partial x_j}(\overline{u_i u_j} = -\frac{1}{\rho}\frac{\partial \bar{p}}{\partial x_i} + v\frac{\partial}{\partial x_j}(\frac{\partial \overline{u_i}}{\partial x_j} + \frac{\partial \overline{u_j}}{\partial x_i}) = -\frac{1}{\rho}\frac{\partial \bar{p}}{\partial x_i} + 2v\frac{\partial}{\partial x_i}S_{ij} \tag{4}$$

The spatial filtering of Navier–Stokes equations eliminate small scales from the flow variables and reduces the computational demands. The impact of the small scales then come into sight at least as subfilter stresses in the momentum equation and as boundary terms. Generally, RANS method (5), (6), (7) is used for the computation of air pollution dispersion.

$$\frac{\partial U}{\partial x_i} = 0 \tag{5}$$

$$\frac{\partial U_i}{\partial t} + \frac{\partial}{\partial x_i}(U_j U_i) = -\frac{1}{\rho}\frac{\partial p}{\partial x_i} + v\frac{\partial^2 U_i}{\partial x_j x_i} + \frac{u_i' u_j'}{\partial x_j} \tag{6}$$

$$u_i = U + u_i' \tag{7}$$

This approach, average the equations in time over all the turbulent scales, to directly generate the statistically steady solution of the flow variables, (Breuer et al. 2003; Franke et al. 2004). Similar to LES the averaging produce additional terms in the momentum equation known as the Reynolds stresses which express the effects of the turbulent fluctuations on the averaged flow. This term has to be modeled. This is the charge of the turbulence models, which will be discussed in the next section.

The unsteady RANS (URANS) has been introduced to capture the dynamics of turbulent complex flows using reasonable computational costs. To have incompressible flow the Navier–Stokes equations have been time-filtered: all scales smaller than a characteristic time period (t) are averaged. The time period should be orders of magnitude higher than the time scale of the random fluctuations, and the averaging period must be much lower than the time scale of the unsteady mean motion (Sadiki et al. 2006).

2.2 Turbulence Models

A turbulence model describes the turbulent fluxes or Reynolds stresses as a function of the mean flow variables, (Franke et al. 2004). The standard two-equations model is the linear k-ε model (8), (9), (Murakami 2002).

$$\frac{\partial(\rho k)}{\partial t} + \frac{\partial(\rho k u_i)}{\partial x_i} = \frac{\partial}{\partial x_j}\left[\frac{\mu_t}{\sigma_k}\frac{\partial k}{\partial x_j}\right] + 2\mu_t E_{ij}E_{ij} - \rho\varepsilon \tag{8}$$

$$\frac{\partial(\rho \varepsilon)}{\partial t} + \frac{\partial(\rho \varepsilon u_i)}{\partial x_i} = \frac{\partial}{\partial x_j}\left[\frac{\mu_t}{\sigma_\in}\frac{\partial \varepsilon}{\partial x_j}\right] + C_{1\in}\frac{\varepsilon}{k}2\mu_t E_{ij}E_{ij} - C_{2\in}\rho\frac{\varepsilon^2}{k} \tag{9}$$

It is known to produce excellent results in wind engineering applications, (Castro 2003). The major problem of this model is the overproduction of turbulent kinetic energy in regions of stagnant flow. More advanced k-ε models like the renormalization group (RNG) k-ε model of Yahot et al. (1992), or the realizable k-ε model of Shih et al. (1995). These models reduce the stagnation point anomaly without leading to bad results in the wake. Recent developments tend also to indicate that the shear stress transport (SST) version of the k-ω model provides a significant improvement over standard k-ε models. See for example, (Menter 1997) and (Menter et al. 2003).

2.3 Dispersion Modeling

Numerous models are accessible to predict the dispersion of the airborne material. In this study, only the species transport module is used. By the resolution of a convection-diffusion equation for the ith species, CFD codes calculate the mass fraction of each species, Yi. This conservation equation takes the following general formula.

$$\frac{\partial}{\partial t}(\rho Y_i) + \nabla \cdot (\rho \vec{v} Y_i) = -\nabla \cdot \overrightarrow{J_i} + R_i + S_i \tag{10}$$

3 Configuration Description, Meshing, Boundaries Conditions and Numerical Setup

3.1 Geometry

The dimensions of the computational domain were 600 m length of 580 m width by 200 m height inside of which the buildings are located. The geometry was performed

Fig. 1 Hanover geometry
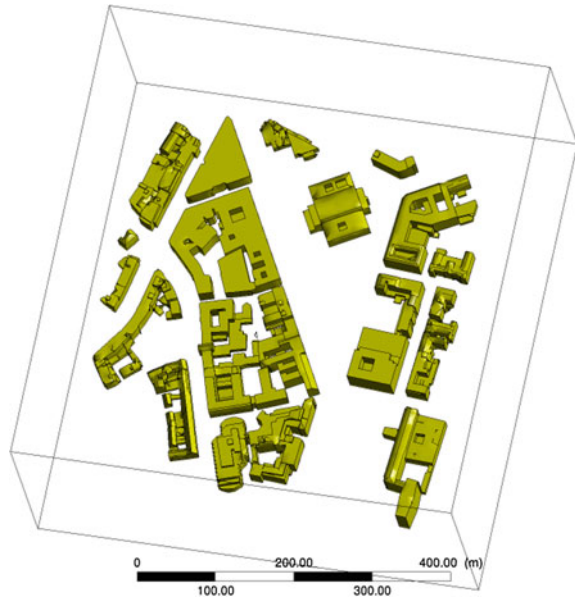
with any space claim then was repaired where necessary and defeatured to assist both the fluid domain extraction and the meshing process. Figure 1 depicts the computational domain used to simulate the configuration of Hannover city. It includes various building having different dimensions and showing multiples features. Streets in the configuration demonstrate unequal dimensions and changeable direction.

3.2   Computational Grid

We have generated two mesh having 19 and 40 million elements in 10 h. An appropriate refinement near the source of CH_4 and close to the ground was performed. Figure 2 exhibit the mesh used for Hannover simulations. The grid quality is improved while increasing the cell number. It should be proved that obtained results are statistically independent of the mesh refinement. This condition implies that many test cases involving different refining degree are to be tested for each operating conditions.

3.3   Boundaries Conditions

The wind velocity is considered an important input parameter for the study of heavy gas dispersion. In a realistic atmosphere, wind commonly does not flow at the same
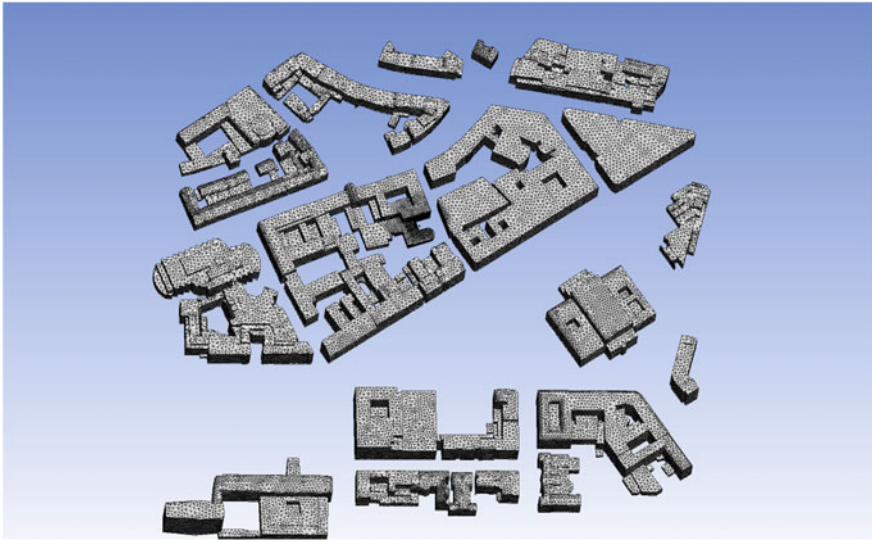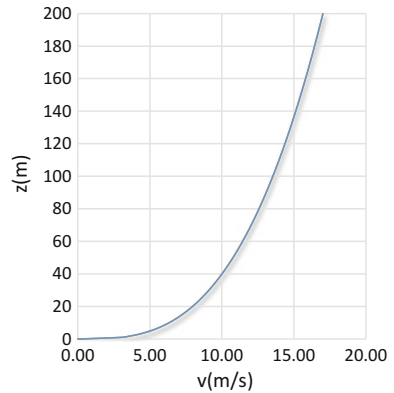
Fig. 2 Hanover unstructured mesh

Fig. 3 Velocity profile at inlet boundary

velocity at different heights due to the frictional effect of the ground. Generally, the power law profile is shown in Fig. 3 is used to describe the variation in the wind speed as a function of the height in the surface boundary layer. $v(z) = v_r k z^a$, V_r is the wind velocity at a standard height of 10 m. As to the pollutant inflow, CH_4 was emitted into a grid space through the stack, which is a square with a length of 1 m. The injected CH_4 was of 100% purity. The CH_4 outlet velocities from the stack were 8 m/s, all the boundary and initial conditions are summarized in Table 1. The types of boundary conditions are shown in Fig. 4

Table 1 Boundaries conditions type

Parameters	Boundary type
Inlet	Velocity inlet of air
Origin	Velocity inlet of CH_4
Bottom	Wall
Top, outlet	Pressure outlet
Left, right	Symmetry
Air temperature	300 k
CH_4 temperature	273 k
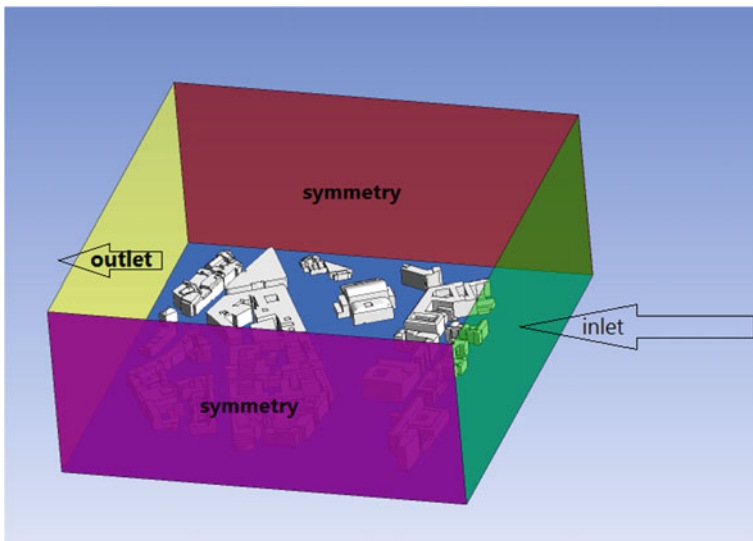
Fig. 4 Geometry with boundaries

4 Results and Discussion

Results were presented in terms of contours of velocity, pollutant concentration, and streamlines. Quantitative results are available and can be plotted.

Two different scenarios are investigated in the configuration of Hannover. In the first, one leakage of CH_4 is introduced through an opening located at the center of the computational domain, i.e., in a confined geometry. The choice of this location is based on its closeness to buildings and long distance far from the exit flow. CH_4 is injected with different inlet velocities horizontally toward the building. Effect of air and methane temperature on the dispersion of CH_4 is investigated. The flow direction, i.e., vertically or horizontally is also studied. The second leakage scenario focuses on the dispersion of methane within an open surface, i.e., ,along with the street and far from the building. Simulations show significant different results.
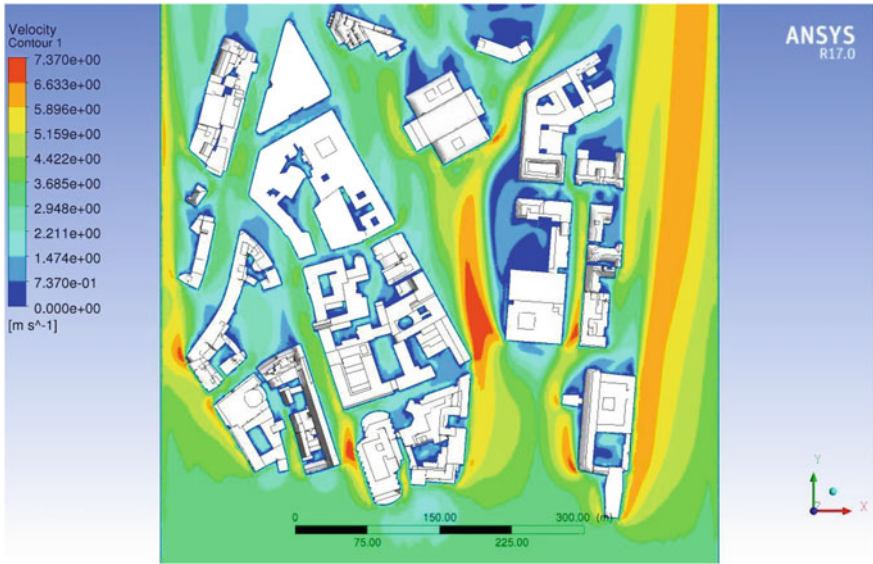
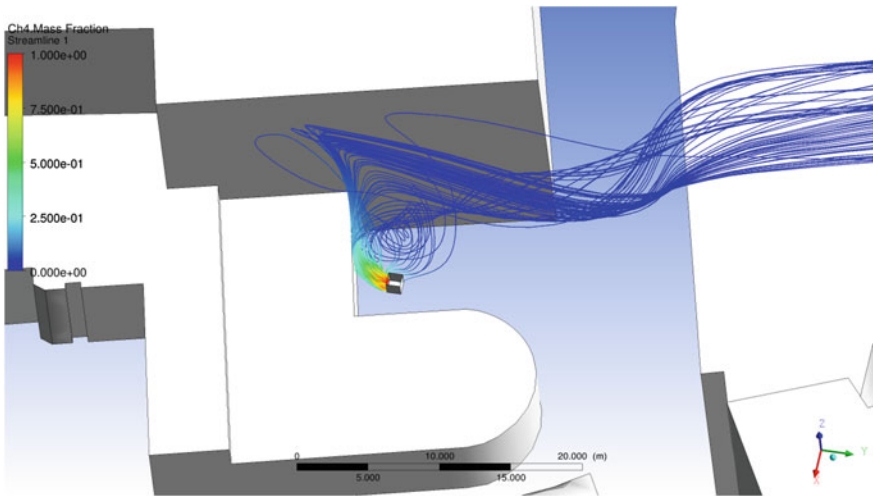**Fig. 5** Velocity profile z = 3 m

Fig. 6 Streamlines from pollution source

Figure 5 shows the velocity contour in a level 3 m high from the ground. The maximum velocity magnitude, 7.3 m/s, is located at the central street, which is the narrowest throat along the street. This can be explained by the conservation of mass. As the flow is incompressible high velocity is likely the most important parameter that controls species transport and dispersion. Behind some building
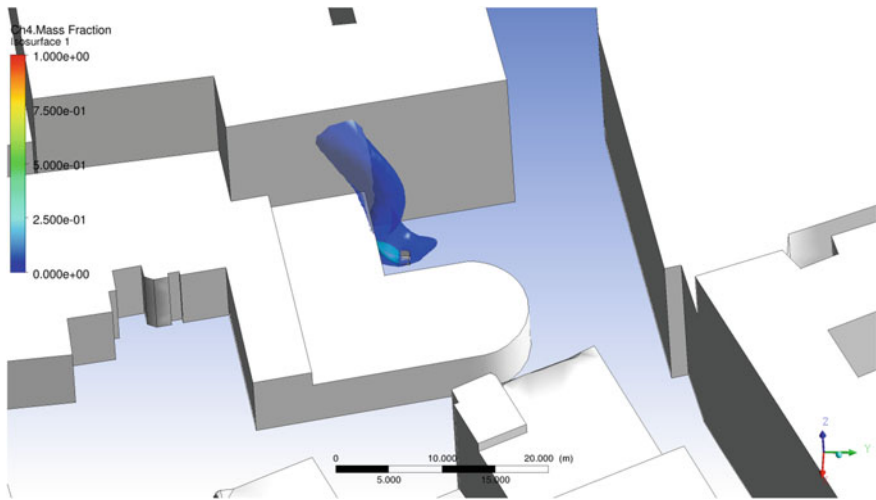
Fig. 7 Isosurface concentration

stagnating fluid is noticed. Figure 6 depicts streamlines derived from the CH_4 inlet. Through methane is introduced horizontally toward the wall, it promptly changes the direction and moves vertically, then it is transported by the carrier air to the outlet. The vertical transport is induced by the buoyancy force. Different densities cause the lighter gas be moved to the top. Methane is 64% lighter as air in the same temperature. Simulations with a temperature of air and CH_4 of 30 °C and 0 °C, respectively, did not alter the dispersion of methane. A vertical flow of CH_4 as inlet direction even increase the transport of methane away from the ground. The dispersion is driven, in this location, by the buoyancy and gravitation forces. Worth to notice that air exhibits an almost null velocity close to the ground.

Figure 7 demonstrates isosurfaces of CH_4 concentrations. Two isovalues are shown, these are C = 0.04 and 0.4. These values represent the flammability limits in case of combustion. The burnable mixture of methane and air shows a vertical plume. The mixture reaches the wall of the nearby building. Parts of it are in touch with the ground. The concentration changes rapidly from 100% CH_4 into less than 4%.

Figure 8 depicts the iso-concentration of methane. Using CFD, it is possible to predict the source of CH_4 if measurements are carried out at the exit boundary. One observes that methane diffuse in the lateral direction as well, i.e., the plume of the isosurface gets wider toward the outlet. This dispersion is more induced by the turbulent and kinematic diffusion. At the outlet, the methane does not climb into the atmosphere considerably.

Figure 9 shows the temperature contours of isosurface close to the CH_4 inlet. CH_4 Rapidly increase the temperature and reaches 300 K which is the temperature
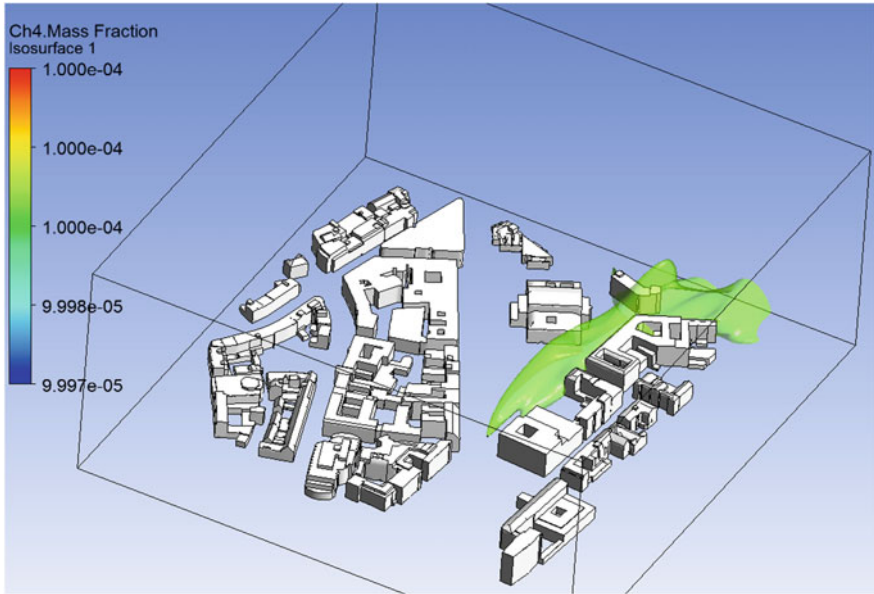
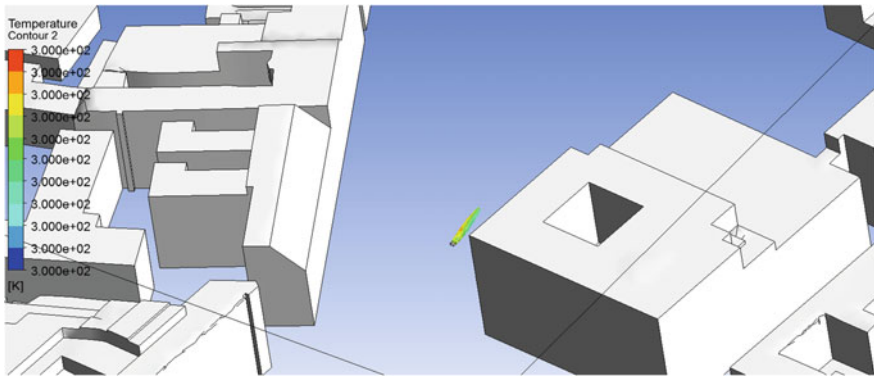**Fig. 8** CH$_4$ isosurface showing the transport of methane species

Fig. 9 Temperature contours of CH$_4$ and air mixture

of ambient air. Simulations with different temperature differences between air and methane reproduced very similar results hinting that thermal variation is not affecting CH$_4$ dispersion. The heat capacity of methane is twice larger as air, therefore, thermal equilibrium is registered in the vicinity of CH$_4$ leakage. Thus, air and CH$_4$ temperatures have no impact on the mixture development and pollutant dispersion.

5 Conclusion

CFD is applied to predict pollution dispersion and species transport in urban cities. Sources CH_4 is being introduced in the computational domain at different locations in the ground and variable altitude in height. Introduced pollutants are injected in different directions and velocity magnitude, i.e., different boundary conditions. The temperature of pollutants and surrounding air at the initial and boundary conditions are also considered as changeable parameters.

The geometry, of Frankfurt having a diameter of 600 m, which includes many building and skyscrapers that demonstrate complex feature and different topology as well as a 600 m $\times$ 580 m urban district from Hannover is numerically investigated and different boundary conditions scenarios are predicted. Two turbulence models, i.e., realizable k-e (RANS) and Large Eddy Simulation (LES) are applied to capture the effect of turbulence and velocity fluctuation in time and space. Worth to mention that LES predicts flow dynamics and mixture development better than RANS. Furthermore, LES is able to capture fluid structure and flow unsteadiness. Yet the computational cost is manifold time larger than RANS. The numerical grid for both configurations included 40 million control volumes, which need a huge computational power. The meshing resolve regions with important velocity gradients and high curvature using the fine grid. It is mandatory to capture at least 80% of turbulence using LES. Increasing the computational domain will necessitate the increase of mesh resolution. The computational power needs to be increased as well. One should note that throughout the literature it is very rare that researcher exceeds 40 million control volumes in CFD simulations.

The applied boundary conditions for ambient air at the inlet used a logarithmic profile that mimics the air velocity in the experimental conditions. The profile varies as a function of the vertical location "z" and is calibrated using two constant parameters.

The configuration of Hannover revealed two important informations, the namely CH_4 dispersion is controlled by air-CH_4 density ratio in case of pollutant injection close to the building. The buoyancy forces are responsible for the stratification of gases. CH_4 species are first transported in the vertical direction then moved by the carrier phase to the outlet. The velocity direction and magnitude, as well as the temperature difference between CH4 and ambient air, do not play important roles.

If CH_4 is injected far from building, i.e., in the middle of the street, a location in which carrier phase velocity is important, then the transport of pollutant showed different behavior. CH_4 is dragged horizontally much faster in the vertical direction. Simulations were able to clearly predict streamline stemming from CH_4 inlet. They followed the street and keep almost a constant altitude until reaching the outlet.

References

Blocken B, Janssen W, van Hooff T (2012) CFD simulation for pedestrian wind comfort and wind safety in urban areas: general decision framework and case study for the Eindhoven university campus. Environ Model Softw 30:15–34

Breuer M, Jovii N, Mazaev K (2003) Comparison of DES, RANS and LES for the separated flow around a flat plate at high incidence. Int J Numer Meth Fluids 41(4):357–388

Castro IP (2003) CFD for external aerodynamics in the built environment. QNET-CFD Netw Newslett 2(2):4–7

Chan TL, Dong G, Leung CW, Cheung CS, Hung WT (2002) Validation of a two dimensional pollutant dispersion model in an isolated street canyon. Atmos Environ 36:861e872

DeCroix D, Brown M (2002) Report on CFD model evaluation using URBAN 2000 field experiment data. Technical report. IOP 10, LA-UR-02-4755. Available from Los Alamos National Laboratory

Franke J, Hirsch C, Jensen A, Krus H, Schatzmann M, Westbury P, Miles S, Wisse J, Wright N (2004) Recommendations on the use of CFD in wind engineering, COST Action C14. European Science Foundation COST Office

Huber A, Georgopoulos P, Gilliam R, Stenchikov G, Wang S, Kelly B, Feingersh H (2004) Modeling air pollution from the collapse of the world trade center and assessing the potential impacts on human exposures. In: Environmental manager Feb 2004, pp 35–40

Kikumoto H, Ooka R (2012) A numerical study of air pollutant dispersion with bimolecular chemical reactions in an urban street canyon using large-eddy simulation. Atmos Environ 54:456–464

Menter F (1997) Eddy viscosity transport equations and their relation to the k-ε model. J Fluids Eng 119:876–884

Menter FR, Kuntz M, Langtry R (2003) Ten years of industrial experience with the SST turbulence model. In: Hanjalic K, Nagano Y, Tummers M (eds) Turbulence, heat and mass transfer, vol 4. Begell House Inc

Moin P, Mahesh K (1998) Direct numerical simulation: a tool in turbulence research. Annu Rev Fluid Mech 30(1):539–578

Murakami S (2002) Setting the scene: CFD and symposium overview. Wind Struct 5(2–4):83–88

Rudman M, Blackburn H (2006) Direct numerical simulation of turbulent non-Newtonian flow using a spectral element method. Appl Math Model 30(11):1229–1248

Sadiki A, Maltsev A, Wegner B, Flemming F, Kempf A, Janicka J (2006) Unsteady methods (URANS and LES) for simulation of combustion systems. Int J Therm Sci 45(8):760–773

Salim SM, Ong KC, Cheah SC (2011) Comparison of RANS, URANS and LES in the prediction of air flow and pollutant dispersion. In: Proceedings of the world congress on engineering and computer science 2011 WCECS 2011, vol II. 19–21 Oct 2011

Shih T-H, Liou WW, Shabbir A, Yang Z, Zhu J (1995) A new k-ε eddy-viscosity model for high reynolds number turbulent flows—model development and validation. Comput Fluids 24 (3):227–238

Tang W, Huber A, Bell B, Kuehlert K, Schwarz W (2005) Application of CFD simulations for short-range atmospheric dispersion over the open fields of project prairie grass. In: Air and waste management association 98th annual conference, June 21–23 Paper No. 1243, Minn

Tominaga Y, Stathopoulos T (2010) Numerical simulation of dispersion around an isolated cubic building: model evaluation of RANS and LES. Build Environ 45(10):2231–2239

Wendt J, Anderson J, for Fluid Dynamics VKI (1996) Computational fluid dynamics: an introduction. Von Karman Institute book. Springer

Yakhot V, Orszag SA, Thangam S, Gatski TB, Speziale CG (1992) Development of turbulence models for shear flows by a double expansion technique. Phys Fluids A 4:1510–1520